

## **Urban Runoff Peak Frequency Curves**

**J. Marsalek**

Hydraulics Div., National Water Research Institute,  
Burlington, Canada

Runoff peak frequency curves were derived from runoff flows observed in an urban test catchment and from runoff flows simulated for storms selected from two rainfall records. The first record, of a shorter length, was recorded in the test catchment. The second rainfall record, of a greater length, was recorded at a station located 10.6 km west of the test catchment. Comparisons of peak frequency curves derived from observations and both sets of simulations indicated a good agreement. As the sewer system became surcharged, the rate of flow increase with the increasing return period diminished.

### **Introduction**

Determination of urban runoff peak frequency curves, which serve for the design of drainage systems, is one of the most important tasks of urban hydrology. One of the tools for determination of runoff peak frequency curves is simulation of rainfall/runoff processes for selected rainfall inputs and catchment conditions. Ideally, a continuous simulation model should be used to produce a simulated runoff record which would be then subject to frequency analysis to derive the runoff peak frequency curves. Continuous simulation, which may be tedious in terms of input data preparation and expensive in terms of simulation costs, is sometimes approximated by a series of discrete-event simulations. Although such simulations

are most often done for synthetic design storms (Arnell 1982), uncertainties in design storms led to the proposal to use historical storms in design applications (Marsalek 1977, Johansen and Harremoës 1979). In this procedure, the rainfall record is screened for events with high runoff potential, runoff hydrographs are simulated for these events by means of an event model adjusted for initial catchment conditions and subject to frequency analysis (Marsalek 1978; Walesh, Lau and Liebman 1979). Advantages of a series of discrete-event simulations arise from lower input data requirements, lower computer costs, and the feasibility of using common runoff models for this purpose.

Acceptability of discrete-event runoff simulations as opposed to continuous simulation was discussed by various researchers (Linsley and Crawford 1974). Much of the criticism of discrete-event simulations was transposed from studies of natural catchments where the catchment flood potential is undoubtedly controlled by the antecedent moisture conditions. The processes controlling runoff are quite different in fully urbanized catchments. For relatively short return periods, which are used in minor drainage design (say 2-5 years), the generation of runoff peaks is primarily controlled by the impervious parts of the catchment. This is particularly true for catchments with a certain minimum imperviousness (greater than 10%) and well-drained soils. Consequently, the conditions pertaining to the pervious part of the catchment, such as the antecedent moisture conditions, become of secondary importance and may be approximated in discrete-event simulations without any significant loss of reliability of results.

In the paper that follows, the runoff peak frequency curves are derived from simulated runoff events and compared to the curve derived from peaks which were observed in a test catchment. Such comparisons serve to confirm the viability of using discrete-event simulation to derive runoff peak frequency curves and also to demonstrate the ability of the employed runoff model to reproduce runoff events of widely varying return periods.

### **Test Catchment Description**

Runoff simulations were undertaken for the Malvern test catchment which is located in Burlington, Ontario. The catchment has been described in detail elsewhere (Marsalek 1979) and only the basic catchment parameters are summarized below.

The Malvern urban test catchment (see Fig. 1) is a residential subdivision of 23.31 ha which is drained by storm sewers. The catchment served for monitoring of rainfall and runoff from 1973 to 1977. The catchment inclines gently from the north boundary line towards the drainage outlet in the southwest corner. The overall catchment surface slope is about 1%. Local slopes, however, depend on

## Urban Runoff Peak Frequency Curves

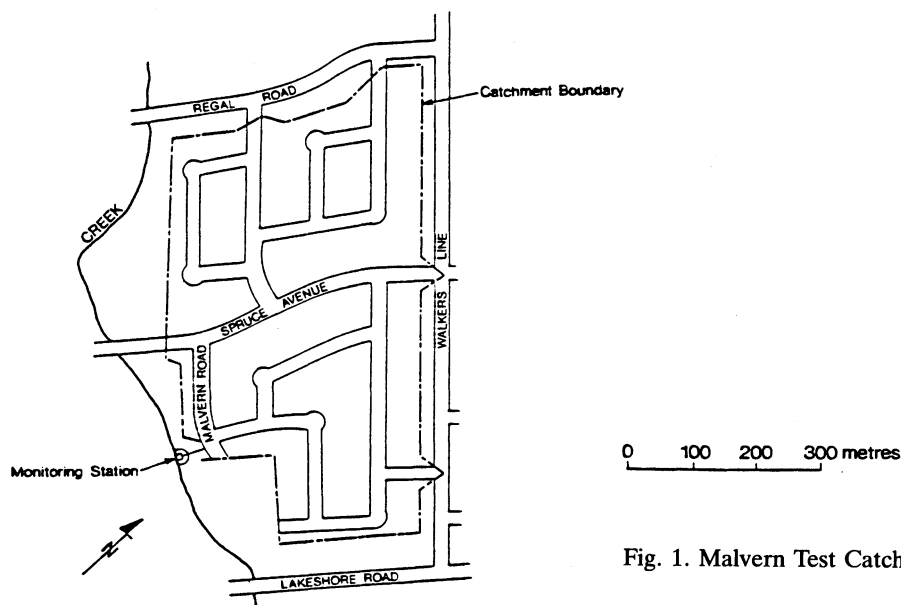


Fig. 1. Malvern Test Catchment.

the grading of individual lots. Front yards typically incline towards streets with slopes varying from 2 to 10%. Backyards incline away from streets towards drainage swales which run along the back line of lots.

Impervious segments of the catchment include roofs, roads, driveways and sidewalks. The total area of impervious parts of the catchment was estimated as 8.16 ha, thus yielding the catchment imperviousness of 35%. With the exception of sidewalks (0.66 ha), all the impervious parts drain directly into storm sewers. The sidewalks drain either on driveways or on a narrow grass strip which separates them from streets.

The pervious, grass-covered parts of the catchment amount to 15.15 ha. The soil can be classified as a well-drained Fox sandy loam. Limited point measurements of infiltration yielded the infiltration values of about 120 mm/hr for dry soil conditions.

The Malvern catchment is served by a tree type, converging storm sewer system which is shown in Fig. 2. The sewer sizes vary from 0.25 m to 0.84 m at the outfall. All the sewers are made of standard concrete pipes which are in a relatively good condition. The sewer system was designed for a discharge of 1.362 m<sup>3</sup>/s at the outfall. It appears that the system can convey a 2-year runoff peak without surcharging.

Details of the Malvern catchment instrumentation were given elsewhere (Marsalek 1979). The monitoring station included a recording rain gauge and a flow measuring weir installed at the outfall. The rain gauge was a standard tipping

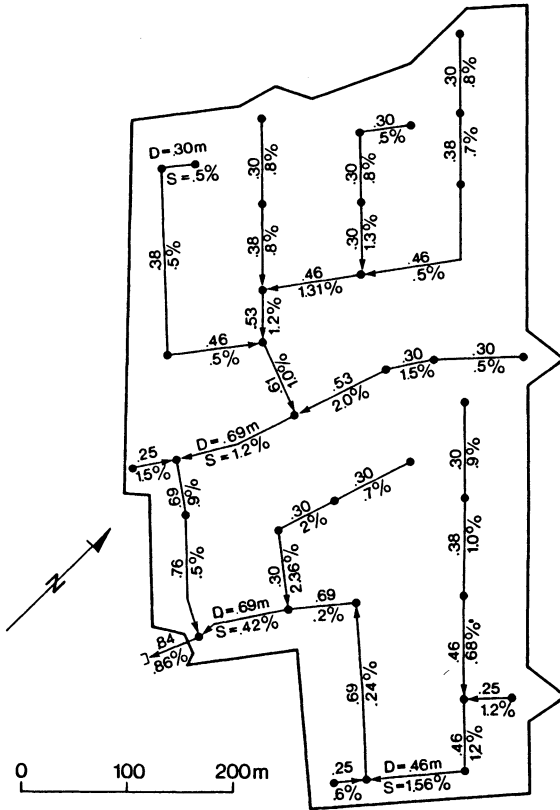


Fig. 2. Malvern Storm Sewer System.

bucket with the capacity of 0.25 mm. The rectangular measuring weir, which was installed in a weir box attached to the drainage outfall, remained operational even when the outfall pipe was surcharged. The accuracy of flow measurements was estimated as  $\pm 5\%$ .

**Rainfall-Runoff Data Base**

The rainfall-runoff data base used in this study consisted of rainfall and runoff data which were observed at the Malvern catchment and of rainfall data from the meteorological station at the Royal Botanical Gardens (RBG) in Hamilton. The RBG station is located about 10.6 km west of the Malvern catchment. The interest in the RBG data followed from the greater length of the RBG record – 15 years as opposed to five years in the case of the Malvern station. Although great differences in hyetographs were noticed for individual storms recorded at both stations, the general rainfall characteristics which are rather conservative should be similar

## Urban Runoff Peak Frequency Curves

Table 1 – Top-Ranked Runoff Events Observed in the Malvern Test Catchment.

Rank	Storm No.	Observed Peak Discharge (m <sup>3</sup> /s)	Estimated Return Period (years)
1	12	1.744	6
2	3	1.608	3
3	13	1.218	2
4	31	1.212	1.5
5	26	1.202	1.2
6	27	1.099	1.0
7	15	1.079	0.86
8	4	1.031	0.75
9	19	1.021	0.67
10	17	0.993	0.60
11	14	0.947	0.55
12	1	0.907	0.50

at both stations. For example, the Intensity-Duration-Frequency (IDF) curves for the RBG station (10.6 km west for Malvern) and for the Oakville OWRC station, which is 11.6 km east of the Malvern catchment, are practically identical. It would appear that the maximum rainfall intensities at the Malvern catchment may be characterized by the IDF curves which are available for the RBG station.

### Malvern Runoff Peak Flows

The monitoring of runoff flows at the outfall from the Malvern catchment was continuous during the field season which spanned from April to December. Because the high runoff peaks were produced by summer thunderstorms, it may be safely assumed that the seasonal records collected contain top-ranked events.

During the monitoring period from 1973 to 1977, about 300 rainfall/runoff events were monitored. Most of these events were rather minor. For the purpose of this study, only 12 events with top-ranked runoff peaks were selected for further analysis. The return periods of these events were calculated from the Weibull's formula as  $T = (N+1)/R$ , where  $N$  is the record length in years and  $R$  is the rank of the peak flow. Furthermore, storm rainfall hyetographs were prepared for runoff simulations. The average rainfall depth of these 12 storms was 18.4 mm and the mean peak 5-minute intensity was about 70 mm/hour. A list of the selected events is given in Table 1.

### Rainfall Data From the RBG Station

A 15-year rainfall record was available for the RBG station which is operated by the Atmospheric Environment Service. This record was screened to identify the storms that were likely to produce high runoff peaks. For this purpose, all storms

with either a total rainfall depth greater than 12.5 mm or a 10-minute peak intensity greater than 15 mm/hour were identified. A total of 54 storms met one or both of these criteria. Next, the top 20 storm rainfall depths were identified for durations of 5, 10, 15, 30, and 60 minutes. Because a number of storms contained multiple maxima, this segregation process yielded only 27 storms that met all the selection criteria. For the purpose of establishing the frequency of occurrence of runoff peaks in the catchment studied, these 27 storms were regarded as a suitable replacement for the 15-year rainfall record. The basic characteristics of these 27 selected storms were given elsewhere (Marsalek 1978). A brief summary of these characteristics follows.

In the segregation of storms, the minimum inter-event time was taken as three hours. That is, a storm event was defined as one where at least three hours without rainfall occurred before and after the event. On this basis, the average total rainfall depth was 33 mm and the average storm duration was about six hours for the storms selected. The mean peak 5-minute intensity was 75 mm/hour.

The relationship between the antecedent dry-weather period and the antecedent five-day precipitation of these heavy storms was also of interest. The mean antecedent dry period was about four days and the five-day antecedent precipitation was 11.5 mm. Because the values of these parameters indicated that the catchment studied is fairly dry at the onset of heavy storms, the neglect of the effects of antecedent precipitation on runoff from the associated storms appeared to be an acceptable approximation. This observation, which is supported by the comparisons of observed and simulated flows presented later, confirms the feasibility of obtaining reliable results from discrete-event runoff simulations.

## **Runoff Simulations**

Simulations of urban runoff in the Malvern catchment were done by means of the Storm Water Management Model of U.S. Environmental Protection Agency, Version III, dated September, 1981. The Storm Water Management Model (SWMM) has been described in detail elsewhere (Huber, Heaney, Nix, Dickinson and Polman 1982) and, consequently, the discussion here is limited to a few important model features.

The SWMM model consists of a number of blocks which can be used in various combinations, depending on the nature of the problem under investigation. The generation of runoff and runoff routing through simple sewer networks without surcharging or special hydraulic structures is accomplished by the RUNOFF block. In more extensive sewer networks with special hydraulic features and free flow, the sewer flow routing is accomplished by means of the TRANSPORT block. Finally, the sewer flow routing in surcharged systems with special hydraulic

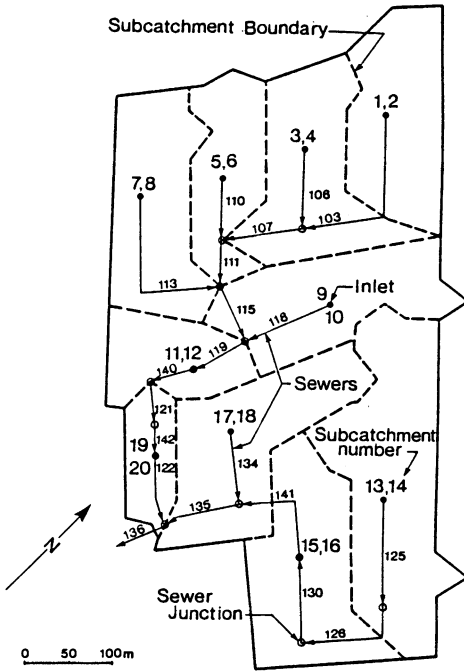


Fig. 3. Test Catchment Discretization.

structures is accomplished by means of the EXTRAN model. As the sophistication of the routing model increases, so do the computer processing times and costs.

Earlier studies indicated (Marsalek 1979) that, for free flow conditions, satisfactory simulations of runoff in the Malvern catchment can be obtained by using the RUNOFF block only. Consequently, the same approach was adopted here. For pressurized flow conditions, it was desirable to use a dynamic flow routing model and, consequently, the EXTRAN model was used to route inlet hydrographs which had been produced by the RUNOFF block.

### Catchment Discretization

For modelling purposes, the Malvern catchment was subdivided into 20 paired subcatchments. Such discretization followed the earlier work with 10 subcatchments which were further subdivided by separating the backyards from the rest of the subcatchment area. Such an arrangement was deemed beneficial for proper modelling of runoff from backyards whose contributions should be relatively small (fully pervious areas) and delayed because of the long flow route. The general outline of subcatchment boundaries is shown in Fig. 3; the basic characteristics of subcatchments are given in Table 2.

The characteristics which were common for all the subcatchments were determined in the earlier studies (Marsalek 1979) as follows:

Table 2 – Subcatchment Characteristics.

Subcatchment Number	Area (ha)	Width (m)	Percent Impervious
1	1.30	853	62.0
2	0.98	161	0.0
3	1.59	1042	60.5
4	0.93	153	0.0
5	1.25	821	61.8
6	0.32	52	0.0
7	1.60	1052	60.9
8	0.83	136	0.0
9	1.11	731	65.5
10	1.36	224	0.0
11	0.80	523	58.9
12	0.56	92	0.0
13	1.87	1225	62.5
14	1.97	323	0.0
15	1.35	888	63.5
16	1.33	218	0.0
17	1.30	853	64.8
18	2.00	328	0.0
19	0.78	513	62.7
20	0.08	14	0.0

*Slope:* 0.03 for subcatchments with impervious segments

0.02 for fully pervious subcatchments

*Overland flow roughness:* described by Manning's  $n=0.013$  for impervious segments, 0.30 for pervious segments

*Depression storage:* 0.5 mm for impervious segments, 9.4 mm for pervious segments

*Infiltration rates (after Horton):*  $f_{\max} = 127$  mm/hour,  $f_{\min} = 13.2$  mm/hour, and the decay rate  $K = 0.00115$  s<sup>-1</sup>.

Additional discussion of subcatchment parameters follows.

Subcatchment areas were derived from a map of the catchment and from drainage patterns. It should be recognized that the catchment imperviousness derived from maps contained some uncertainties arising from measurement and sampling errors. Furthermore, the connectivity of impervious elements was not always clear, because some of the elements drained onto pervious elements and barely contributed to the catchment runoff. It was therefore desirable to verify the catchment imperviousness, which was derived from the map, against the value obtained from observed volumetric runoff coefficients. Such verification was undertaken



## Urban Runoff Peak Frequency Curves

for intermediate rainfall/runoff events during which all the runoff was generated on impervious elements. This condition may be expressed as

$$V_{ru} = A_{imp} (h-d) \tag{1}$$

where  $V_{ru}$  is the runoff volume,  $A_{imp}$  is the total area of contributing impervious elements,  $h$  is the rainfall depth, and  $d$  is the depression storage. By dividing both sides of Eq. (1) by the catchment area,  $A$ , the following expression is obtained

$$h_{ru} = i (h-d) \tag{2}$$

where  $h_{ru} = V_{ru}/A$  is the runoff depth, and  $i = A_{imp}/A$  is the catchment imperviousness. Thus by plotting  $h_{ru}$  versus  $h$  for a number of events, a straight line will be obtained and the slope of this line represents the effective catchment imperviousness. Such a procedure was followed using nine intermediate events from the 1975 data (see Fig. 4). The slope of the regression line was 0.346. Such a value is within the range of values (0.32-0.35) which were determined from the map for the directly-connected and total impervious areas, respectively.

The subcatchment width in the SWMM model represents the physical width of the overland flow. According to the SWMM manual (Huber et al. 1982), the widths of individual subcatchments were taken as twice the main sewer pipe length. The slope of subcatchments is not particularly important, because the simulated runoff peaks are barely sensitive to the surface slope, within practical limits (Proctor&Redfern Ltd. and James F. MacLaren 1976). The chosen values were 0.03 and 0.02 for subcatchments with impervious elements and for backyard subcatchments, respectively. Such slopes reflect the average local slopes (lot grading, road and roof slopes) rather than just the overall catchment slope.

The roughness of subcatchment surfaces was characterized by the Manning's  $n$  and the appropriate values were selected from the SWMM manual (Huber et al. 1982). Depression storage on impervious areas was determined in the earlier studies. For pervious areas, the value adopted was slightly higher (by 3 mm) than the SWMM default value, in order to reflect low surface slopes and possible water

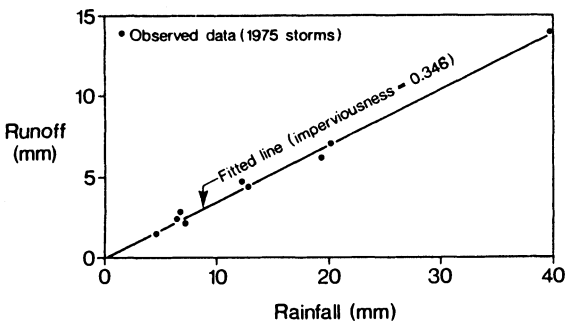


Fig. 4. Calibration of Catchment Imperviousness.

ponding in backyards.

Finally, the infiltration capacities were selected on the basis of limited field measurements and the soil description (sandy loam). It is believed that, for the storms studied, the integrated Horton's infiltration capacity equation used in the SWMM III model makes the simulated runoff peaks less sensitive to the choice of Horton's parameters than the earlier non-integrated form of the same equation.

**Sewer Network**

The Malvern sewer network was represented in two ways – in a simplified form adequate for open-channel flow routing in the RUNOFF block and in a comprehensive form which is required for pressurized flow routing in the EXTRAN model. Descriptions of both forms follow.

For simulations with the RUNOFF block, the Malvern sewer network was approximated by 19 sewer pipes ranging in diameter from 0.305 m to 0.84 m. Inlets to the sewer system were placed close to the centroids of individual subcatchments. Small-diameter pipes (less than 0.305 m) were neglected. Such a loss of pipe storage volume was partially compensated for by increasing the diameter of three pipes (Nos. 106, 110, and 140) along the route from the inlet to the downstream subcatchment boundary. This was done to avoid sewer surcharging which could result from allowing the entire subcatchment outflow to enter through the inlet. In the actual system, the subcatchment runoff enters the sewer at a number of points along the pipe and only the sewer section at the downstream subcatchment boundary is designed to convey the entire subcatchment runoff. Thus, the maximum diameter of the sewer draining the subcatchment was extended upstream to the subcatchment inlet. Besides the diameter, the sewer pipes were also characterized by their length, slope, and roughness. A summary of sewer characteristics is given in Table 3; the sewer layout is shown in Fig. 5.

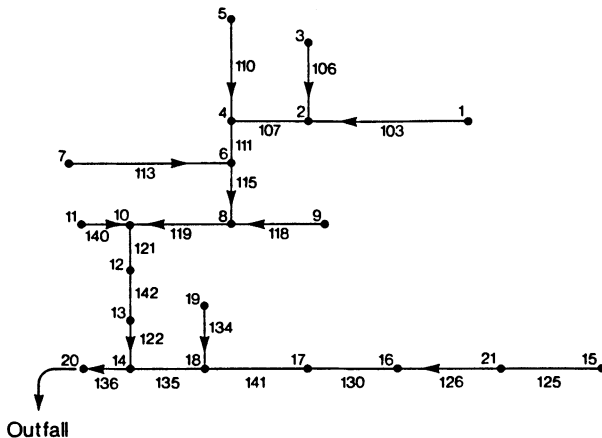


Fig. 5. Schematized Sewer Layout for Pressurized Flow Routing.

## Urban Runoff Peak Frequency Curves

Table 3 – Characteristics of the Sewer Network Used in EXTRAN Flow Routing.

Pipe No.	<i>D</i> (m)	Length (m)	Slope	<i>t<sub>c</sub></i> (s)	Junction Head Loss Coeff.	Data Invert Drop (m)	Equivalent Manning's <i>n</i>
103	.458	209	.0051	98.6	1.2	0.00	0.0146
106	.305 <sup>1</sup>	91	.0132	52.6	1.2	0.19	0.0148
107	.458	91	.0132	42.9	1.4	0.11	0.0155
110	.381 <sup>1</sup>	122	.0120	63.1	0.2	0.15	0.0141
111	.534	57	.0120	24.9	0.4	0.08	0.0148
113	.458	192	.0050	90.6	2.2	0.53	0.0151
115	.610	74	.0100	30.3	1.2	0.70	0.0162
118	.534	107	.0200	46.7	0.2	0.15	0.0142
119	.686	117	.0120	45.1	1.4	0.06	0.0146
140	.458 <sup>1</sup>	54	.0120	25.5	1.2	0.49	0.0161
121	.686	57 <sup>2</sup>	.0090	22.0	0.2	0.00	0.0136
142	.763	64 <sup>2</sup>	.0050	23.4	0.2	0.00	0.0118
122	.763	81	.0050	29.6	1.4	0.24	0.0171
125	.458	125	.0156	59.0	1.6	0.22	0.0149
126	.458	125	.0156	59.0	0.8	0.22	0.0144
130	.686	92	.0024	35.5	0.2	0.00	0.0144
141	.686	134	.0024	51.7	1.2	0.00	0.0155
134	.305	89	.0236	51.5	0.2	1.71	0.0148
135	.686	85	.0042	32.8	0.6	0.15	0.0152
136	.839	62 <sup>2</sup>	.0086	21.6	0.3	0.00	0.0141

<sup>1</sup> A slightly larger diameter was used in RUNOFF block simulations

<sup>2</sup> The pipe length was increased (roughness reduced) to increase *t<sub>c</sub>*

For pressurized flow routing with EXTRAN, the sewer system was defined as a set of nodes (sewer junction manholes) which were connected by links (sewer pipes). In total, 21 nodal points and 20 connecting links were considered. The nodal points were described by junction invert elevations, ground surface elevations at junctions, and the connections of subcatchment outlets. Sewer pipe parameters had to be slightly modified as required by numerical solutions employed in the EXTRAN model. In particular, the longest conduit should not exceed the shortest one by more than five times (Roesner, Shubinski and Aldrich 1982). It was therefore necessary to shorten the original pipe No. 125 by inserting a node and dividing this pipe into two.

In order to establish the computational time step, the time of travel of surface waves through individual conduits, *t<sub>c</sub>*, was calculated as

$$t_c = \frac{L}{\sqrt{gD}} \tag{3}$$

where  $L$  is the conduit length,  $D$  is the conduit diameter, and  $g$  is the acceleration due to the gravity. The selected computational time step should then be shorter than  $t_c$ 's calculated for all the conduits. A preliminary calculation indicated that a computational time step of 20 seconds would be realistic for all conduits except Nos. 121, 136 and 142 which produced slightly shorter times of travel of surface waves. Consequently, these conduits were replaced by their equivalents which were longer but smoother in order to maintain the same time of flow travel. Thus for the equivalent conduits, the times calculated from Eq. (3) were increased, but the flow travel times remained the same. The roughness of the equivalent conduits was calculated from the following formula (Roesner, Shubinski and Aldrich):

$$n_e = \frac{n_p (L_p)^{\frac{1}{2}}}{(L_e)^{\frac{1}{2}}} \tag{4}$$

where  $n$  is the Manning's roughness, and the subscripts  $e$  and  $p$  refer to the equivalent and prototype conduits, respectively. As recommended in the EXTRAN manual, the prototype conduit roughness was taken as  $n_p=0.014$ .

For pressurized flow routing, it was desirable to account for head losses at sewer junctions. Although this can not be done directly in the EXTRAN model, junction head losses can be compensated for by increasing the conduit roughness. The junction head loss,  $h_j$ , can be expressed as

$$h_j = K \frac{v^2}{2g} \tag{5}$$

where  $K$  is the loss coefficient and  $v$  is the mean flow velocity.

The conduit friction head loss,  $h_c$ , can be expressed as  $h_c=S_cL$ , where  $S_c$  is the friction slope. The equivalent head loss,  $h_{eq}$ , which accounts for both the junction and friction head loss, can be written as

$$h_{eq} = h_j + h_c \tag{6}$$

and after substituting for  $S_c$  from the Manning's equation, the following expression is obtained for the equivalent conduit roughness  $n_{eq}$ :

$$n_{eq} = \sqrt{n_p^2 + 0.008 \frac{K D^{1.33}}{L}} \tag{7}$$

where  $n_p$  is the prototype roughness, and both  $D$  and  $L$  are given in metres. Junction head loss coefficients and the equivalent conduit roughness coefficients, which were calculated from Eq. (7), are listed in Table 3. This table also contains the upstream conduit heights above the junction invert. These differences in invert elevations are used to compensate for junction head losses.

## *Urban Runoff Peak Frequency Curves*

The EXTRAN model can simulate various special hydraulic structures in the sewer system. The only such structure in the Malvern system was the measuring weir at the outfall. This weir was included in EXTRAN simulations by specifying the weir height, length, and discharge coefficient as input data for simulations.

### **Simulation Procedures**

Simulations of runoff from the Malvern catchment were undertaken for the selected Malvern and RBG storms. Such simulations were done with the SWMM III model which was operated in the discrete event mode. Considering the low antecedent rainfalls of the events studied, no adjustments of model infiltration parameters were deemed necessary and all the simulations were done for dry antecedent conditions. The computational time step was selected as two minutes. Such a time step coincided with the rainfall discretization interval and was used successfully in earlier studies of the Malvern catchment.

Whenever sewer surcharging was detected in simulations with the RUNOFF block, a new simulation was done using both the RUNOFF block and the EXTRAN model. In that case, the RUNOFF block was used to produce inlet hydrographs which were then routed through the sewer system by the EXTRAN model. The flow routing time step was 20 seconds. The maximum number of iterations was selected as 30 and the surcharged flow tolerance was 5%. Both these values were adopted from the EXTRAN manual (Roesner, Shubinski and Aldrich 1982).

### **Results and Discussion of Results**

The simulation results are presented and discussed in two parts – first the results for the Malvern events and then the results for the RBG events.

The return periods of the top 12 runoff peaks observed in the Malvern catchment were estimated in the range from 0.5 to 6 years. Although the observation record length is relatively short (5 years) for conventional frequency analysis, it should be recognized that the urban minor drainage systems are designed for short return periods (two years in the studied case) and, in this regard, the length of the record used here is adequate.

Malvern runoff hydrographs were simulated for all 12 events. The simulated peak flows are listed in Table 4 and plotted in Fig. 6. In general, a fairly good agreement between the observed and simulated peaks was obtained. The mean value of the ratio of the observed peaks to simulated peaks was 1.03 with a standard deviation of 0.23. The difference between the observed and simulated peaks had a mean value of  $-0.009 \text{ m}^3/\text{s}$  with a standard deviation of  $0.206 \text{ m}^3/\text{s}$ .

Runoff peak flows were then used to produce peak frequency curves for both

Table 4 – Runoff Peaks Simulated for the Malvern Catchment.

Storm No.	Sim. Peak Discharge (m <sup>3</sup> /s)	Est. Return Period (years)	Storm No.	Sim. Peak Discharge (m <sup>3</sup> /s)	Est. Return Period (years)
3	1.892	6	123	2.043	16
12	1.824	3	144	1.944	8
26	1.481	2	125	1.898	5.33
31	1.433	1.5	120	1.765	4
13	1.395	1.2	102	1.694	3.20
15	1.109	1.0	146	1.646	2.67
14	1.096	0.86	108	1.623	2.29
1	1.064	0.75	110	1.580	2.00
6	1.015	0.67	139	1.419	1.78
4	0.964	0.60	147	1.402	1.60
17	0.813	0.55	101	1.375	1.45
27	0.798	0.50	136	1.368	1.33
			131	1.300	1.23
			106	1.269	1.14
			135	1.265	1.07
			132	1.201	1.00
			129	1.177	0.94
			154	1.124	0.89
			137	1.080	0.84
			115	1.014	0.80

observations and simulations (see Fig. 6). For visual guidance, regression lines for both observed and simulated peak curves were also plotted in Fig. 6. The agreement between both regression lines is quite good, because errors in individual peaks are smoothed out in the curve fitting procedure. Note also that in the frequency analysis, the ranks of observed and simulated peaks do not coincide for individual events.

Initial simulations for the Malvern events which produced the three largest peaks indicated surcharging in the sewer system. Consequently, runoff simulations were repeated for these events using the EXTRAN model for pressurized flow routing. The agreement between the observed and simulated peaks was fairly good for these events and fully comparable to that obtained for less intense events with free flow in the sewer system.

In order to extend runoff simulations to the region of longer return periods, the RBG storms were also applied to the Malvern catchment. In this case, the estimated return periods of simulated peaks ranged from 1 to 16 years and the top 10 events had to be processed by using the EXTRAN model for flow routing. The

## Urban Runoff Peak Frequency Curves

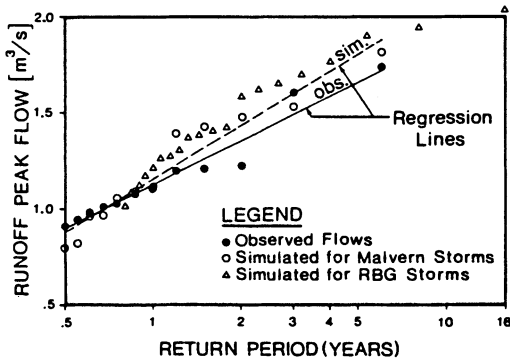


Fig. 6. Observed and Simulated Runoff Peak Flows.

simulated peak flows are listed in Table 4 and plotted in Fig. 6. A fair agreement between the flows simulated for the Malvern and RBG events is apparent from Fig. 6.

It was of interest to note that the slope of the frequency curve for the RBG storms gradually decreased with the increasing return period and the degree of sewer surcharging. Such a change was not found in the earlier simulations with free flow routing and suppressed surcharging (Arnell 1982). As the sewer system surcharges, the hydraulic grade line starts to rise above the conduit crowns and, eventually, it will reach the ground surface at junctions and water will start to overflow from sewer system at manholes. This condition then imposes an upper limit on the sewer system capacity. This limiting condition is reached earlier in simulations, if the head losses considered include both pipe friction and sewer junction head losses. For example, for the longest flow route in the Malvern system passing through the junctions 1-4-8-10-14-20 (see Fig. 5), the calculated junction head losses represented almost 20% of the total head loss.

For design flow conditions (i.e. a 2-year return period), the total head loss along the aforementioned route was calculated as 8.3 m. The head drop available between the inverts of junctions 1 and 20 was 7.68 m or, if the maximum head available is taken as the difference between the ground surface elevation at junction 1 and the pipe crown elevation at junction 20, the value of 8.82 m is obtained. Thus the system is adequately designed to convey the design flow with a possible minor surcharging. For a 5-year return period, the maximum flow velocities exceeded, for limited duration, the design velocities by about 50% and the corresponding head losses more than doubled in comparison to the design situation. Such head losses would then lead to water overflow from the system at junction manholes and would limit the discharge at the catchment outfall.

It was also noted that the frequency curves for Malvern and RBG storms agreed fairly well, although both stations are about 10.6 km apart and individual storms observed at both sites on same days showed significant differences. Such differences were randomly distributed and thus did not affect much the frequency

curves. Any storm observed at both Malvern and RBG stations would have different characteristics and generally produce different simulated runoff peaks of different return periods. The agreement between frequency curves simulated for Malvern and RBG data suggests that the general runoff-producing properties of rainfall data from both stations are fairly conservative in space and such properties then control the runoff frequency curves. This finding which is so far limited to the data discussed here indicates the feasibility of using a single rainfall record to develop historical or synthetic design storms for the entire municipality, provided that there are no orographic effects present.

### **Summary and Conclusions**

Runoff peak frequency curves were produced for a fully urbanized catchment from five years of observations and from runoff simulations for storms observed in the catchment and at another station 10.6 km west of the catchment. The simulations were performed by means of the calibrated SWMM III model and, whenever sewer surcharging was encountered, the pressurized flow routing was accomplished by means of the EXTRAN model. The most important parameter for the calibration of runoff peaks was the catchment imperviousness which was calibrated by a regression analysis of observed rainfall and runoff volumes. Observed runoff hydrographs indicated that in the Malvern catchment, which can be characterized by an intermediate imperviousness and well-drained soils, the pervious areas barely contributed to the generation of runoff peaks with return periods up to five years.

The study results indicate that, with a calibrated model, runoff frequency curves can be derived from discrete-event runoff simulations with a better accuracy than that typically achieved for individual events. This follows from the fact that random errors in individual simulated peak flows are reduced in plotting and curve-fitting procedures.

The SWMM model reproduced the observed runoff peaks fairly well. The agreement between the observed and simulated peaks of return periods from one to six years was comparable to that reported earlier for fairly frequent events. Such an agreement was obtained for dry antecedent conditions which seem to represent the normal antecedent conditions in the study area. These results further confirm the feasibility of using design storms for establishing design runoff flows, provided that the normal antecedent conditions are specified. Such findings may be limited to the catchments similar to the Malvern catchment. In catchments with low imperviousness and poorly drained soils, the soil infiltration would play a much more significant role.

The EXTRAN model performed satisfactorily in pressurized flow routing. For



## Urban Runoff Peak Frequency Curves

proper simulation of head losses in the sewer network, head losses at sewer junctions were approximated by increasing the adjacent conduit roughness. It was noticed that the slope of the runoff peak frequency curve decreased in the pressurized flow region. For longer return periods, the sewer systems becomes severely surcharged and water overflows out of the system at junction manholes.

### References

- Arnell, V. (1982) Rainfall Data for the Design of Sewer Pipe Systems. Report Series A:8, Dept. of Hydraulics, Chalmers University of Technology, Göteborg.
- Huber, W. C., Heaney, J. P., Nix, S. J., Dickinson, R. E., and Polman, D. J. (1982) Storm Water Management Model User Manual – Version III. Dept. of Environmental Engineering Sciences, University of Florida, Gainesville, Florida.
- Johansen, L., and Harremoës, P. (1979) The Use of Historical Storms for Urban Drainage Design. Proc. International Symposium on Urban Storm Runoff, University of Kentucky, Lexington, pp. 61-70.
- Linsley, R., and Crawford, N. (1974) Continuous Simulation Models in Urban Hydrology. *Geophysical Research Letters, AGU, Vol. 1, No. 7*, pp. 321-322.
- Marsalek, J. (1977) Runoff Control in Urbanizing Catchments. Proc. of Symposium on Effects of Urbanization and Industrialization on the Hydrological Regime and on Water Quality, IAHS-AISH Publication No. 123, pp. 153-161.
- Marsalek, J. (1978) Research on the Design Storm Concept. Technical Memorandum No. 33, ASCE Urban Water Resources Research Program, New York, N.Y.
- Marsalek, J. (1979) Malvern Urban Test Catchment, Vol. II. Res. Report No. 95, Canada-Ontario Agreement on Great Lakes Water Quality, Environment Canada, Ottawa.
- Proctor&Redfern, Ltd. and James F. MacLaren, Ltd. (1976) Storm Water Management Model Study Vol. I. Res. Report No. 47, Canada-Ontario Agreement on Great Lakes Water Quality Environment Canada, Ottawa.
- Roesner, L. A., Shubinski, R. P., and Aldrich, J. A. (1982) Storm Water Management Model User's Manual Version III, Adendum I – EXTRAN. Municipal Environmental Research Laboratory, U.S. Environmental Protection Agency, Cincinnati, Ohio.
- Walesh, S. G., Lau, D. H., and Liebman, M. (1979) Statistically-Based Use of Events Models. Proc. International Symposium on Urban Storm Runoff, University of Kentucky, Lexington, pp. 75-81.

Received: 27 March, 1984

*J. Marsalek*

**Address:**

J. Marsalek,  
National Water Research Institute,  
867 Lakeshore Road,  
Burlington, Ontario L7R 4A6,  
Canada.